Polymeric Gadolinium Chelate–Containing Magnetic Resonance Signal-Enhancing Coating Materials: Synthesis, Characterization, and Properties

Jian Guo, Xiqun Jiang, Chang-Zheng Yang

College of Chemistry and Chemical Engineering, Nanjing University, Nanjing 210093, China

Received 15 November 2001; accepted 25 March 2002

ABSTRACT: The present investigation deals with studies on novel magnetic resonance signal-enhancing coating materials. The polyaminocarboxylate complexes of Gd^{3+} as side chains were prepared by the conjugation of *N*-(2-hydroxyethyl)ethylenediaminetriacetic acid (HEDTA) with poly(styrene-maleic acid) copolymer (SMA). The complexation of the Gd^{3+} ion to the conjugates was carried out by adding $GdCl_3$ to the solution of the polymer ligands. The resulting Gd^{3+}-containing polymer complexes were characterized by GPC, FTIR, NMR, and inductively coupled plasma–Auger electron spectroscopy, which confirmed that HEDTA was covalently attached to SMA and Gd^{3+}-containing polymer complexes were formed. The PP catheters were coated with the Gd^{3+}-containing polymer complexes and characterized by XPS. The result confirms that the Gd^{3+} complexes were coated on the surface of PP catheters. In the relaxation test, the relaxation rates of the water proton in the vicinity of the coated PP catheter surface increase significantly, suggesting that Gd^{3+}-containing polymer complex coating materials show great MR enhancement of water proton, and potentialities in making catheters used for endovascular interventions or therapy, visible by MRI. The influence of protein on the relaxation rates of coated PP catheter shows that the protein adsorption on the catheter surface influences the enhancement of the MR signal for the coating materials of Gd^{3+}-containing polymer complex.
 J Appl Polym Sci 87: 1358–1364, 2003

Key words: ESCA/XPS; coatings; relaxation

INTRODUCTION

Gd^{3+} chelates are frequently chosen as contrast agents for magnetic resonance imaging (MRI) examination because of the high effective magnetic moment and relatively long electronic relaxation time, which enhance the water proton relaxation rates in the tissues where they distribute.[1–3] In recent years, the potential advantages of macromolecular complexes of Gd^{3+} chelates compared to those of the low molecular weight Gd^{3+} chelates are well recognized. The conjugation of Gd^{3+} chelates to polymeric materials was anticipated to increase the rotational correlation time and, hence, to improve the relaxivity per gadolinium atom.[4] The increased lifetime of the macromolecular complexes as contrast agents in the blood pool has been identified as an important feature in both blood pool and dynamical tumor imaging.[5–7] Combined with tissue-specific targeting molecular agents, these macromolecular Gd^{3+} complexes are also envisioned to be disease-specific contrast agents.[8–10]

We are interested in exploring the use of macromolecular Gd^{3+} complexes as a magnetic resonance signal-enhancing coating material in the field of interventional MR. In the few past years, MRI-guided endovascular therapy has been paid increasing attention because MRI offers many advantages over X-ray–guided methods, with respect to reducing risk and improving surgical outcomes.[11–14] The current limitation of development and application of MRI-guided endovascular therapy is the difficulty in detecting medical devices during imaging because almost all devices (e.g., catheters) do not give rise to imaging in clinical MRI equipment.[15–17] This study reports an investigation on the development of Gd^{3+}-containing polymer complexes that can be coated on the surface of medical devices such as catheters, resulting in sufficient contrast for the catheter to be visualized in the MRI environment.

EXPERIMENTAL

Materials

All solvents used were analytical grade, dried, and distilled before use. Styrene was distilled under reduced pressure over CaH_2. 2,2′-Azobisisobutyronitrile (AIBN) was recrystallized from ethanol. Citric acid was milled and dried at 60°C for 24 h under vacuum. Maleic anhydride was recrystallized from chloroform, and *N*-(2-hydroxyethyl)-ethylenediamine-triacetic acid

Correspondence to: C.-Z. Yang (czyang@nju.edu.cn).

Journal of Applied Polymer Science, Vol. 87, 1358–1364 (2003)

(HEDTA; purchased from Acros Organics Co.) was used without further purification.

Preparation of SMA copolymer

Poly(styrene-maleic acid) copolymer (SMA) was synthesized through solution polymerization initiated by AIBN. Styrene (12.5 g, 12 mmol), maleic anhydride (11.8 g, 12 mmol), and toluene (200 mL) were added to a 500-mL round-bottom flask, and stirred at 60°C to form a clear solution, after which a desired amount of AIBN was added to the solution and the temperature was evaluated to 75–78°C. After the reaction proceeded under vigorous stirring at 78°C for about 2 h, the temperature rose to 80°C and reaction was maintained for an additional hour. After cooling to room temperature, the resultant was filtered off and washed with toluene. The crude product was dispersed into enough toluene again and refluxed for 24 h, filtered off, and washed with toluene. The final product was dried at 80°C under vacuum for 48 h.

Preparation of gd^{3+}-containing polymer complexes

For the preparation of HEDTA–SMA (**1**), the conjugate of HEDTA and SMA, SMA (2.0 g), HEDTA (2.84 g, 10 mmol), *p*-toluenesulfonic acid (0.04 g), and 60 mL dimethyl sulfoxide (DMSO) were added to a 100-mL round-bottom flask equipped with magnetic stirrer, and stirred at 80°C to form a clear yellow solution. The reaction proceeded at 80°C for 12 h under N_2 atmosphere, then cooled to room temperature; the conjugate was precipitated in methanol/water (1 : 4, v/v) and dried at 60°C under vacuum for 24 h.

For the preparation of the Gd^{3+}-containing polymer complexes HEDTA–SMA–Gd (**2**), the copolymer (2.0 g) was dissolved in DMSO and heated to 80°C, after which 0.8 g $GdCl_3$ was added to the solution and stirred for 4 h at 80°C. After cooling to room temperature, the solution was poured into methanol/water (1 : 4, v/v); the precipitation was filtered and washed by water (xylenol orange was used as the indicator to ensure there was no free Gd^{3+} in the water). Finally, the product was dried under vacuum at 60°C for 24 h.

For the preparation of CA–HEDTA–SMA (**3**), the conjugate of HEDTA, citric acid with SMA, and its Gd^{3+}-containing polymer complex CA–HEDTA–SMA–Gd (**4**), the same procedure, as described above, was followed, except that 0.54 g citric acid, 2.13 g HEDTA, and 0.6 g $GdCl_3$ were used.

Coating on the surface of PP catheters

The solution-coating method was used to coat Gd^{3+}-containing polymer complexes on the surface of PP catheters. The PP catheters were polished with sandpaper and ultrasonically cleaned in two successive solutions of tetrahydrofuran (THF), methanol, then treated with silicone coupling agent, KH560, in toluene (5%, w/v). PP catheters (4 mm diameter) were immersed into the Gd^{3+}-containing polymer complex solutions in *N*,*N*-dimethylformamide (DMF). Subsequently, the catheters were placed in the center region of the airproof tubes, and the tubes were evacuated to remove the solvents. The thickness of coating layers that are calibrated based on the weight of the catheters before and after coating can be adjusted by changing this described step several times.

Measurements

The molecular weight and molecular weight distribution of the copolymers were determined by gel permeation chromatography (GPC; Waters 240; Waters Associates, Milford, MA) with polystyrene gel columns at 40°C with DMF as a mobile phase. The molecular weight was calculated by standard procedure on the basis of the universal calibration curve of PS.

Fourier transform infrared (FTIR) spectra were performed with a Bruker IFS 66 FTIR spectrometer (Bruker Instruments, Billerica, MA).

All studies of ^1H nuclear magnetic resonance (NMR) spectra and tests of longitudinal relaxation time (T_1) were performed with a Bruker DPX-300 NMR spectrometer operating at 300 MHz. The sample solution prepared had a concentration of 40 mg/mL in DMSO-d_6.

X-ray photoelectron spectra (XPS) measurements were performed with an ESCALab MK2 apparatus. As a photon source, MgK_α radiation was used, and the X-ray source operated at 15 kV and 20 mA, at an incident angle of 45° and a residual pressure of 1.33×10^{-7} Pa. Surface compositions were calculated for each element from the respective sensitivity and the area of respective photoelectron peak from the spectra.

Inductively coupled plasma (ICP) quantometer measurements were performed with a Jarrell-Ash-1100 ICP–Auger electron spectroscopy (AES) instrument at a pressure of 1.6×10^5 Pa, under an argon atmosphere.

RESULTS AND DISCUSSION

Preparation of gd^{3+}-containing polymer complexes

The preparation of Gd^{3+}-containing polymer complexes was carried out according to **Scheme 1**. SMA was synthesized through solution polymerization of styrene and maleic anhydride initiated by AIBN. To clarify the structure of samples, FTIR spectra and ^1H-NMR spectra were measured. Figure 1 shows the IR spectra of SMA and SMA–HEDTA (**1**). The adsorption bands at 1854 and 1778 cm^{-1} in Figure 1(a) are char-

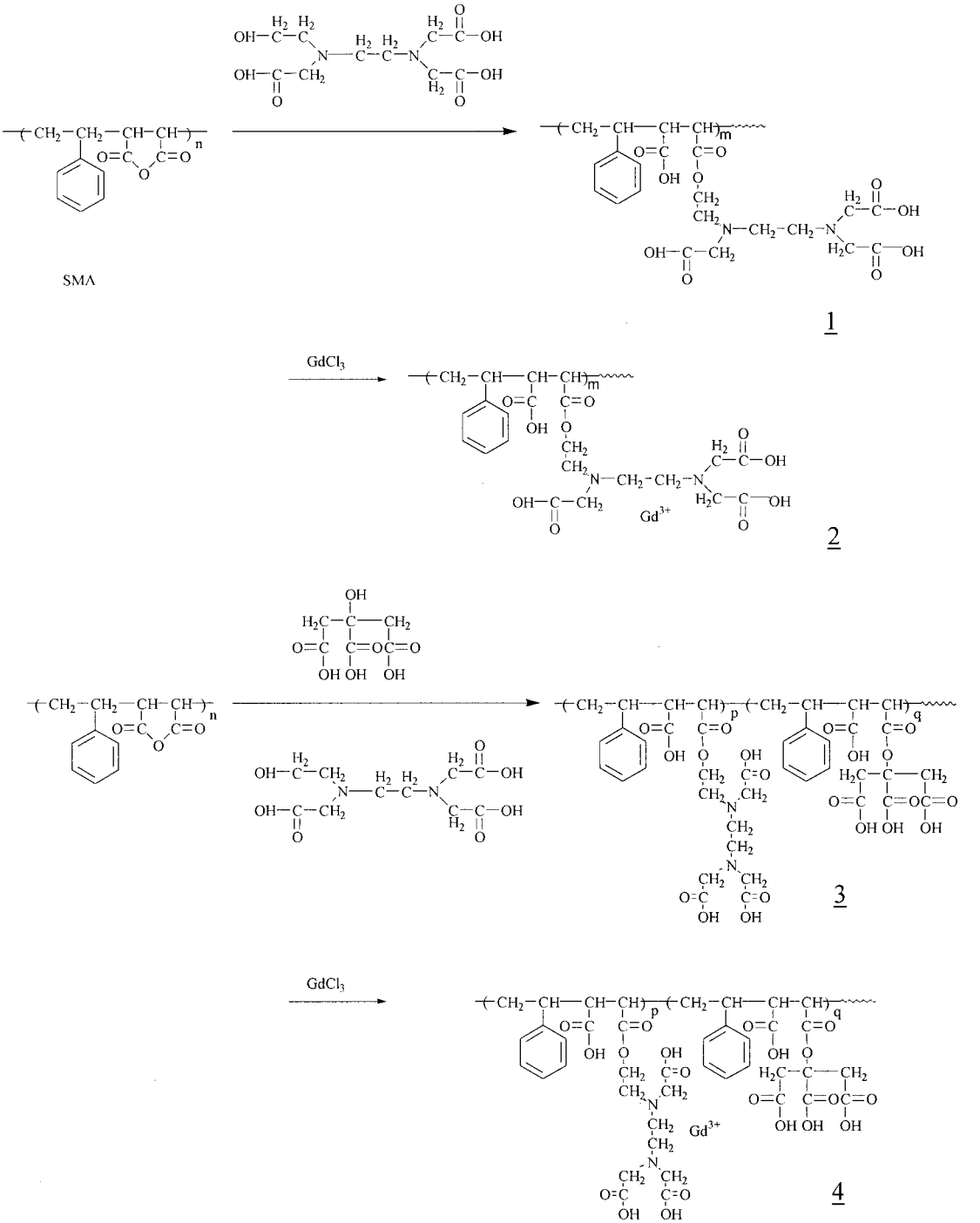

Scheme 1 Synthesis of Gd^{3+}-containing polymer complexes.

acteristic bands of SMA, assigned to asymmetrical and symmetrical vibration $\upsilon_{C=O}$ of maleic anhydride moieties, respectively. The band at 704 cm^{-1} is the $\delta_{C=C}$ of the phenyl groups.[18,19] After the conjugated reaction with HEDTA, Figure 1(b) shows that the C=O stretching vibration band from SMA shifts from 1778 to 1728 cm^{-1}, attributed to the esterification of the maleic anhydride with HEDTA. The adsorption band at 1630 cm^{-1}, which is the characteristic band of HEDTA, is observed, indicating that HEDTA was covalently attached to SMA.

Citric acid is a common blood anticoagulation agent. For modifying the property of coating materials, both citric acid and HEDTA were covalently linked with SMA in the preparation of CA–HEDTA–SMA (**3**). The synthesis was carried out in two steps, First, citric acid was reacted with excessive SMA in the presence of *p*-toluene sulfonic acid and then HEDTA

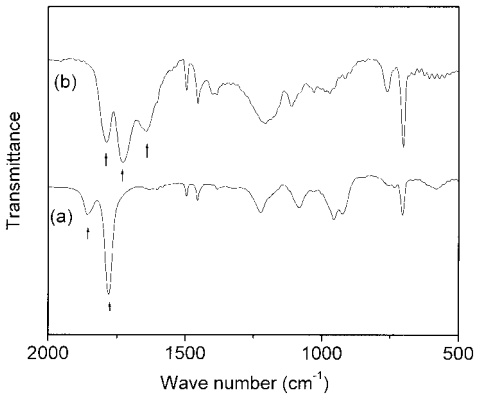

Figure 1 FTIR spectra of (a) SMA and (b) HEDTA–SMA.

was added to the reaction mixture; the mole ratio of citric acid and HEDTA was 1 : 3. Figure 2 shows the FTIR spectra of citric acid–conjugated SMA and **3**. The bands at 1854 and 1778 cm^{-1}in Figure 2(a) correspond to the unreacted maleic anhydride moieties of SMA; the band at 1720 cm^{-1} is attributed to the esterification of SMA with citric acid in the first step. Figure 2(b) shows that, after the reaction with HEDTA, the band at 1854 cm^{-1} disappears and the band at 1630 cm^{-1} occurs, indicating that HEDTA was reacted with residual maleic anhydride in SMA. This result demonstrates that both citric acid and HEDTA were covalently attached to SMA.

Figure 3 shows the ^{1}H-NMR spectra of SMA, HEDTA–SMA (**1**), and CA–HEDTA–SMA (**3**). The chemical shifts at 7.3 ppm, and between 4.0 and 2.2 ppm, are assigned to the phenyl proton and protons from –CH– and $–CH_2–$ groups on the backbone chains as well as HEDTA and citric acid, respectively. The ^{1}H-NMR spectrum in either Figure 3(b) or 3(c) has larger and broader signal peaks between 2.7 and 4.0 ppm compared to those in Figure 3(a). It is well known that

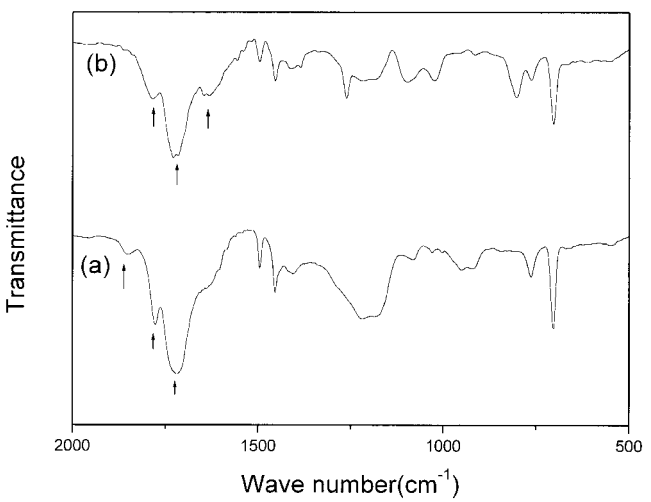

Figure 2 FTIR spectra of (a) citric acid conjugated SMA and (b) CA–HEDTA–SMA.

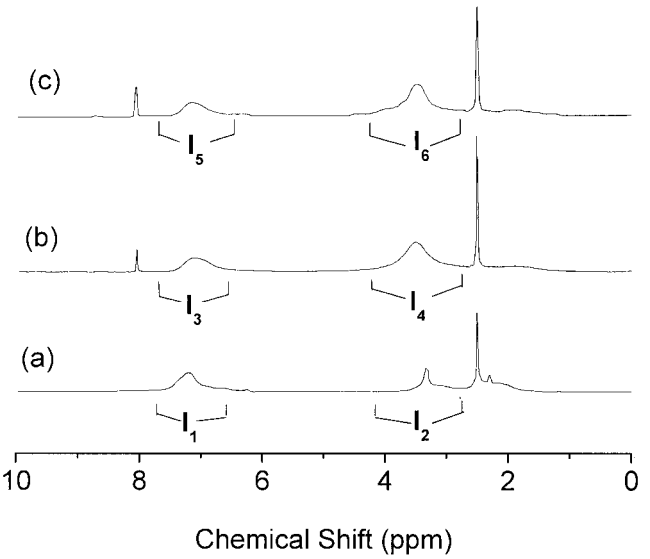

Figure 3 ^{1}H-NMR spectra of (a) SMA, $I_1 : I_2 = 1 : 0.8$; (b) HEDTA–SMA, $I_3 : I_4 = 1 : 2.1$; (c) CA–HEDTA–SMA, $I_5 : I_6 = 1 : 2.0$.

copolymer composition can be determined by comparing the integration intensities of protons. By comparing the ratio of integration intensity of the signal peak at 7.3 ppm assigned to the phenyl group of styrene to the integration intensity of the signal peak between 2.7 and 4.0 ppm, attributed to the –CH– and $–CH_2–$ groups of the backbone chains, HEDTA, and citric acid, the change of chemical composition of SMA before and after the reaction can be obtained. After the conjugated reaction, the integration intensity ratio changes from 1 : 0.8 for SMA to 1 : 2.1 and 1 : 2.0 for **1** and **3**, respectively. This result is in good agreement with the result of FTIR measurement.

The molecular weight of the synthesis copolymers characterized by GPC are summarized in Table I. After the reaction of SMA with HEDTA and citric acid, the M_n of the resulting copolymers **1** and **3** increases to 47,600 and 46,200, respectively. The molecular weight dispersing rate is also increased.

The complexation of the Gd^{3+} to the polymer ligands **1** and **3** was carried out by adding a little less stoichiometric amount of $GdCl_3$ to the solution of the polymer ligand. The characterization was performed by measuring the Gd content in the Gd^{3+}-containing

TABLE I
Characterization of Synthesis Copolymers

Polymer	GPC[a]		
	M_n	M_w	M_w/M_n
SMA	28,000	35,000	1.25
HEDTA-SMA	47,600	86,700	1.82
CA-HEDTA-SMA	46,200	89,600	1.94

[a] Calculated by use of calibration curve for polystyrene.

polymer complexes with ICP-AES; the Gd content in **2** and **4** was 3.75 and 3.24%, respectively.

ESCA measurement of coating on the surface of PP catheters

The PP catheters coated by Gd^{3+}-containing polymer complexes were thoroughly characterized by X-ray photoelectron spectra (XPS). Figure 4 shows the XPS survey spectra of bare PP catheters and coated PP catheters with Gd^{3+}-containing polymer complexes at a takeoff angle of 45°. For a bare PP catheter, two characteristic peaks corresponding to C 1s at 285 eV and O 1s at 532 eV were observed, as shown in Figure 4(a). Neither a nitrogen peak nor a gadolinium peak was detectable. The surface atomic composition for carbon and oxygen was 94.4 and 5.6%, respectively. After coating, the expected characteristic peaks corresponding to N 1s at 400 eV, O 1s at 532 eV, C 1s at 284 eV, and Gd 4d at 146 eV signals were detected, as shown in Figure 4(b) and 4(c). The appearance of a Gd photoelectron peak at the binding energy of 146 eV confirms the chemical attachment of Gd^{3+}-containing polymer complexes on the surface of PP catheters. The relative atomic compositions of PP catheter surfaces are summarized in Table II; these data clearly indicated that the Gd^{3+}-containing polymer complexes were coated on the surface of PP catheters.

Relaxation rates of the gd^{3+}-containing polymer complexes coating on the PP catheter

The most abundant molecular species in biological tissues is water. It is the quantum mechanical spin of the water proton nuclei that ultimately gives rise to the signal in a magnetic resonance imaging experiment. The effect of Gd^{3+} chelate is enhancement of

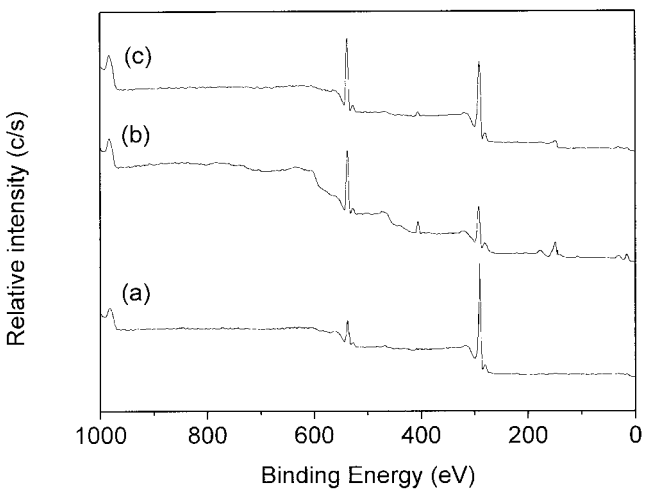

Figure 4 X-ray photoelectron spectra of PP catheter: (a) before coating, (b) coating with HEDTA–SMA–Gd, (c) coating with CA–HEDTA–SMA–Gd.

TABLE II
Surface Chemical Composition of PP Catheters Before and After Coating

	C%	O%	N%	Gd%
Before coating	94.4	5.6	—	—
After coating by **2**	77.4	19.4	3.1	0.81
After coating by **4**	74.9	21.9	2.5	0.74

relaxation rates of water protons in the body's tissues where they distribute. The longitudinal water proton relaxation rate, R_{1obs}, measured for proton in the vicinity of the surface of PP catheter coated by Gd^{3+}-containing polymer complexes **2** and **4**, is 9.08 and 6.36 s^{-1}, respectively. The results indicate that MR signals are significantly enhanced and R_1 relaxation rates increase in the vicinity of the surface of coated PP catheters compared to the R_{1d} value of 0.4 s^{-1}, the relaxation rate of the pure water medium. The ability to enhance the water proton relaxation rates is usually expressed in relaxivity units, r_{1p}, defined as the increase of the water proton relaxation rate in a 1 m*M* solution of the paramagnetic complex, which was calculated from the following equation[1,3]:

$$r_{1p} = \frac{(R_{1obs} - R_{1d})}{[Gd^{3+}]} \quad (1)$$

where R_{1obs} is the observed longitudinal water proton relaxation rate, R_{1d} is the longitudinal relaxation rate of the pure water medium, and $[Gd^{3+}]$ is the concentration of Gd^{3+}. Assumedly, there is no exchange between the inner and outer compartments of the coat of Gd^{3+}-containing polymer complex. The Gd^{3+}-containing polymer complex in the inner compartment does not contribute at all to the observed relaxivity and, therefore, only the portion of the Gd^{3+}-containing polymer complex close to the surface (i.e., in sites accessible to the bulk water) is responsible for the observed relaxation enhancement, as shown in Figure 5. Then, eq. (1) can be written as

$$r_{1p} = \frac{(R_{1obs} - R_{1d})}{[Gd^{3+}]_{outer}} \quad (2)$$

where $[Gd^{3+}]_{outer}$ is the concentration of Gd^{3+} in the outer compartment of the coat. Thus, the actual concentration of Gd^{3+} complex in the outer compartment is very low and the relaxation enhancement caused by this fraction of the Gd^{3+}-containing polymer complex can be deduced to be significantly high.

Influence of protein on the relaxation rates of coated PP catheters

To estimate the impact of protein in the body's blood on the relaxation enhancement and effective lifetime

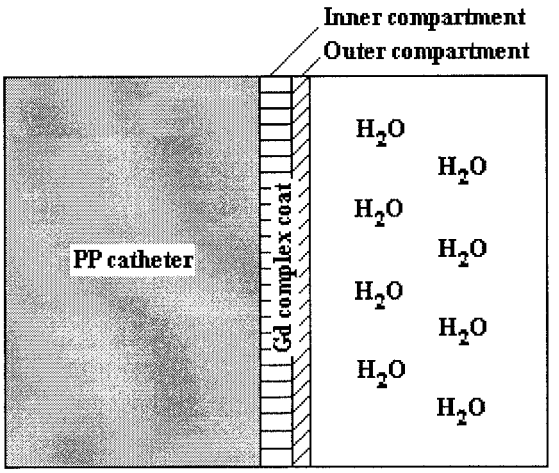

Figure 5 Gd^{3+}-containing polymer complex coating on the surface of PP catheter.

of the coated PP catheter, relaxation rates of coated catheters were measured after they were soaked in bovine serum albumin (BSA) solution. The PP catheters coated by Gd^{3+}-containing polymer complexes were dipped in the solution of BSA (5%, w/v) for the desired time, after which the PP catheters were taken out and placed in the test tubes filled with 50 m*M* phosphate buffer (pH 7.4) for the relaxation rate measurement. Figure 6 shows the relaxation rate R_{1obs} of water proton in the vicinity of the surface of PP catheters, which were dipped in the BSA solution for each different time. The result shows that R_{1obs} decreased along with the prolonged dipping time of PP catheters in BSA solution compared to the R_{1obs} before the dipping. The proton relaxation rate decreased by approximately one half in 15 min.

The possible explanation may be offered to account for this. According to the well-established relaxation theory,[20–22] in principle, in an aqueous solution of a paramagnetic complex, the relaxation enhancement of the solvent water protons is propagated to the bulk through the exchange of the water molecules dipolarly coupled to the metal ion. The water molecule may be directly coordinated to the Gd^{3+} metal ion, or simply diffuse at the surface of the Gd^{3+} complex. The propagation of the paramagnetic effect may occur through (1) the exchange of the coordinated water molecules and/or the exchange of its protons only, (2) the exchange of water molecules hydrogen bonded to polar groups on the complex surface, or (3) the diffusion around the chelate of the water molecules. Although the condition changed here compared to an aqueous solution of Gd^{3+} complex, the relaxation rate of the water proton in the vicinity of Gd^{3+} complex coat is affected by the exchange of the coordinated water molecules with bulk water molecules. Figure 7 shows that, in a model of Gd^{3+} complex coating the film surface, when the PP catheter was dipped in the BSA solution, BSA may aggregate around the surface of the Gd^{3+} complex coat. That may affect the exchange of the bulk water solvent with the coordinated water, especially in the water exchange rate, arising from diffusion of the water molecules near the Gd^{3+} complex coat, resulting in a decrease of relaxation rate in the vicinity of the coated catheter surface.

To make a clear contrast between the catheter and human blood (or tissues), the proton relaxation rate in the vicinity of the surface must be greater than that of the human blood and tissues. Because the protein adsorption on the catheter surface will influence the enhancement of the MR signal for the coating materials of Gd^{3+}-containing polymer complex, the utility will be limited *in vivo*. For example, the MR signal may decrease with the prolonged time. Thus, the reduction of interaction between coating material and protein in blood is very important.

CONCLUSIONS

MR signal-enhancing coating materials were prepared by coordinating Gd^{3+} chelate with SMA copolymer. The PP catheters coated with the coating materials showed great MR enhancement, and the relaxation rates at the surface of the coated samples were shown to increase significantly. It was also found that the relaxation rate of the water proton in the vicinity of the coated catheter surface decreased with increasing the dipping time of coated catheters in BSA solution, which indicates that the protein adsorption on the catheter surface influences the enhancement of the MR signal for the coating materials of Gd^{3+}-containing polymer complex. The reduction of interaction be-

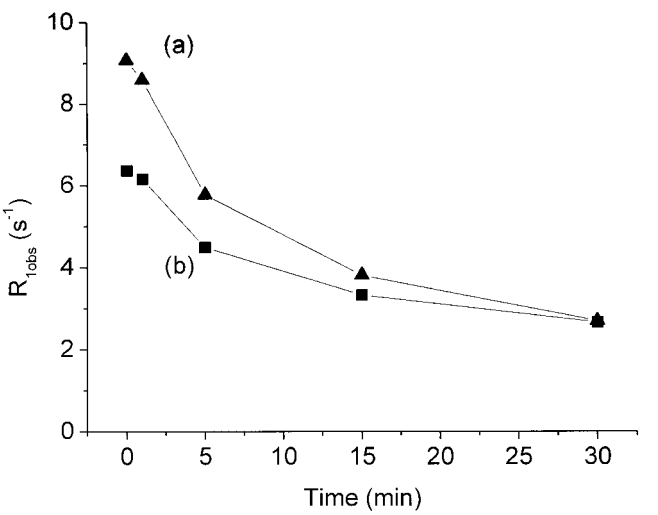

Figure 6 Plot of the relaxation rate of water proton in the vicinity of PP catheters coated by (a) HEDTA–SMA–Gd and (b) CA–HEDTA–SMA–Gd as a function of dipping time in BSA solution.

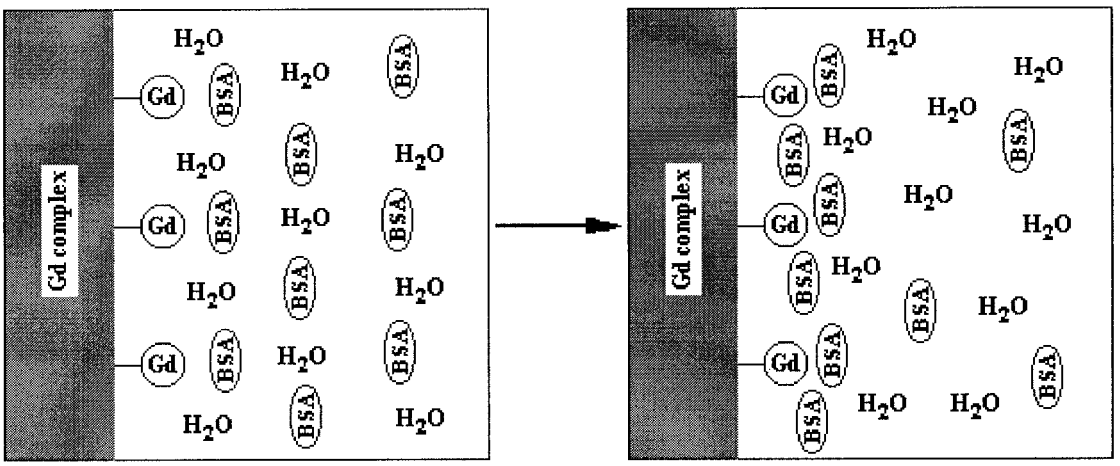

Figure 7 Schematic illustration of aggregation of BSA around the surface of coating material of coated PP catheter.

tween the coating material and protein in blood is extremely important.

References

1. Caravan, P.; Ellison, J. J.; McMurry, T. J.; Lauffer, R. B. Chem Rev 1999, 99, 2293.
2. Aime, S.; Botta, M.; Fasano, M.; Terreno, E. Chem Soc Rev 1998, 27, 19.
3. Lauffer, R. B. Chem Rev 1987, 87, 901.
4. Brasch, R. C. Magn Reson Med 1991, 22, 282.
5. Desser, T. S.; Rubin, D. L.; Fan, Q.; Muller, H. H.; Khodor, S. J Magn Reson Imaging 1994, 4, 467.
6. Ladd, D. L.; Hollister, R.; Peng, X.; Wei, D.; Wu, G.; Delecki, D. Bioconjugate Chem 1999, 10, 361.
7. Robert, H. C.; Saeed, M.; Roberts, T. P. L.; Muhler, A.; Shames, D. M.; Mann, J. S.; Stiskai, M.; Demsar, F.; Brasch, R. C. J Magn Reson Imaging 1997, 7, 331.
8. Aime, S.; Ascenzi, P.; Comoglio, E.; Fasano, M.; Paoletti, S. J Am Chem Soc 1995, 117, 9365.
9. Storrs, R. W.; Tropper, F. D.; Li, Y. H.; Song, C. K.; Kuniyoshi, J. K.; Sipkins, D. A.; Li, K. C. P.; Bednarski, M. D. J Am Chem Soc 1995, 117, 7301.
10. Curtet, C.; Maton, F.; Havet, T.; Slinkin, M.; Mishra, A.; Chatal, J. F.; Muller, R. N. Invest Radiol 1998, 33, 752.
11. Jiang, X.; Yu, H.; Frayne, R.; Unal, O.; Strother, C. M. Adv Mater 2001, 13, 490.
12. Strother, C. M.; Unal, O.; Frayne, R.; Turk, A.; Omary, R.; Korosec, F. R.; Mistretta, C. A. Radiology 2000, 15, 516.
13. Jolesz, F. A. J Magn Reson Imaging 1998, 8, 3.
14. Bakker, C. J. G.; Weber, R. M.; van Vaals, J. J.; Mali, W. T. M.; Viergever, M. A. Radiology 1997, 202, 273.
15. Atalar, E.; Bottomley, A.; Ocali, O.; Correia, L. C. L.; Kelemen, M. D.; Lima, J. A. C.; Zerhouni, E. A. Magn Reson Imaging 1996, 36, 596.
16. Rasche, V.; Holz, D.; Koehler, J.; Proksa, R.; Roeschmann, P. Magn Reson Imaging 1997, 37, 963.
17. Glowinski, A.; Adam, G.; Buecker, A.; Neuerburg, J.; van Vaals, J. J.; Gunther, R. W. Magn Reson Imaging 1997, 38, 253.
18. Wang, M.; Zhu, X.; Wang, S.; Zhang L. Polymer 1999, 40, 7387.
19. Yoshinaga, K.; Sueishi, K.; Karakawa, H. Polym Adv Technol 1996, 7, 53.
20. Koenig, S. H.; Brown, R. D., III. Prog NMR Spectrosc 1990, 22, 487.
21. Aime, S.; Botta, M.; Fasano, M.; Terreno, E. Acc Chem Res 1999, 32, 941.
22. Powell, D. H.; Ni Dhubhghaill, O. M.; Pubanz, D.; Helm, L.; Lebedev, Y. S.; Schlaepfer, W.; Merbach, A. E. J Am Chem Soc 1996, 118, 9333.